Computational and Theoretical Chemistry 983 (2012) 54–60

Contents lists available at SciVerse ScienceDirect

Computational and Theoretical Chemistry

journal homepage: www.elsevier.com/locate/comptc

Theoretical studies of the dependence of nuclear quadrupole coupling constants on intermolecular forces

Agnieszka Brzyska [a], Krzysztof Woliński [a], Michał Jaszuński [b,*]

[a] Department of Chemistry, Maria Curie-Skłodowska University, Maria Curie-Skłodowska sq. 3, 20-031 Lublin, Poland
[b] Institute of Organic Chemistry, Polish Academy of Sciences, Kasprzaka 44, 01-224 Warsaw, Poland

ARTICLE INFO

Article history:
Received 9 December 2011
Received in revised form 29 December 2011
Accepted 29 December 2011
Available online 10 January 2012

Keywords:
Nuclear quadrupole coupling
DFT
Intermolecular forces

ABSTRACT

We study the performance of density functional methods in the calculation of nuclear quadrupole coupling constants (NQCCs), focusing on the effects of weak intermolecular forces. We begin with an analysis of isolated molecule values, comparing the density functional theory (DFT) results for uracil and thymine obtained by applying 11 different functionals with the Møller–Plesset second-order perturbation theory (MP2) values and with accurate experimental data. Next, using a subset of these DFT functionals we examine the interaction-induced changes of NQCCs for weak solute–solvent interactions, with the solvent effect described as a function of the dielectric constant; for adenine–thymine and guanine–cytosine complexes, in which we observe significant effects due to proton transfer in the hydrogen bonds, and for a hexamine complex in the solid state. Three applied DFT functionals provide a similar, satisfying description of the influence of intermolecular forces on the quadrupole coupling constants, in particular when hydrogen bonding leads to large changes of these constants.

1. Introduction

Numerous properties characterizing the interactions between molecules and electromagnetic fields can be successfully computed applying modern methods of quantum chemistry [1]. For example, the parameters applied to interpret the Nuclear Magnetic Resonance (NMR) and Nuclear Quadrupole Resonance (NQR) spectra, such as shielding constants, spin–spin coupling constants and nuclear quadrupole coupling constants (NQCCs), correspond to molecular properties which describe the changes of the electronic structure in the presence of internal and/or external perturbing fields and may be predicted from theory. We shall consider in this work the interaction between the nuclear electric quadrupole moment and the electric field gradient (EFG) at the nucleus, described by the nuclear quadrupole coupling (NQC) tensor.

For isolated small molecules the nuclear quadrupole coupling can be accurately determined from state-of-the-art calculations; moreover, a combined analysis of ab initio and spectroscopic results was used to provide improved values of electric quadrupole moments for many nuclei (see e.g. Refs. [2,3]). However, the comparison of theoretical results with those deduced from NMR and NQR spectra requires an analysis of the effects due to intermolecular forces—the experimental data are usually obtained in the condensed phase. This makes practically impossible a direct comparison with very accurate ab initio results (for instance obtained applying coupled cluster reference wave functions), because the systems properly modeling intermolecular interactions are too large. Consequently, in our study of the role of intermolecular interactions we shall focus on the density functional theory (DFT), and compare its performance with ab initio methods less expensive than the coupled cluster approach—the Hartree–Fock (HF) and the Møller–Plesset second-order perturbation theory (MP2) approximations. It has been established long ago that DFT methods can be successfully applied to describe NQCC; however, the approach often used relied on scaling of the results—an effective value of the nuclear quadrupole moment was determined (for instance, for ^{14}N ca. 5% smaller than the real one, see Refs. [4,5]). We do not follow this approach, it would not be appropriate to apply or optimize a scaling factor and analyse the effects of intermolecular forces at the same time.

2. Computational details

The parameters applied in NQR to analyse the spectrum are given by the components of the NQC tensor defined in its own principal axis system. In particular, the nuclear quadrupole coupling constant is proportional to V_{zz}, the largest component of the diagonalised EFG tensor. The NQCCs are determined according to the standard formula $\chi_{zz} = -eQV_{zz}$, with the following values of the electric quadrupole moments for the nuclei studied in this work: $Q(^{14}\mathrm{N}) = 20.44$, $Q(^{2}\mathrm{H}) = 2.860$ and $Q(^{17}\mathrm{O}) = -25.58$ mb [6]. We shall

* Corresponding author.
E-mail address: michaljz@icho.edu.pl (M. Jaszuński).

2210-271X/$ - see front matter © 2012 Elsevier B.V. All rights reserved.
doi:10.1016/j.comptc.2011.12.022

also discuss the asymmetry of the tensor, defined as $\eta = |(\chi_{xx} - \chi_{yy})/\chi_{zz}|$.

The calculations at the HF, MP2 and DFT levels of theory were carried out using two basis sets: 6-311G-dp and aug-cc-pCVTZ. To estimate the performance of different methods and functionals in the evaluation of NQCC we used at each level of the calculation the same equilibrium molecular geometries, which we have optimized at the B3LYP/6-311G-dp level. We note that for molecules in the solid state other methods may be more suitable for the comparison of the results with experiment, for instance experimental geometries of a central molecule in a cluster (e.g. based on X-ray data) have been used.

Most of the calculations were performed using the PQS program [7]. In addition, Gaussian 09 [8] was used for COSMO/MP2 calculations and CFOUR [9] for a few test CCSD calculations.

3. Results and discussion

3.1. Isolated molecules

We computed the electric field gradient (EFG) in a series of five molecules: uracil, guanine, thymine, cytosine and adenine (see Fig. 1 for atom numbering). These nucleic acid bases molecules have been a subject of a number of experimental and theoretical studies because of their biological significance (see e.g. Refs. [10–21]). However, benchmark NQCC results from microwave spectroscopy of isolated molecules are available only for two molecules, uracil [13,14] and thymine [15], and only for the nitrogen nuclei. Therefore, we first performed the DFT calculations with 11 different exchange/exchange correlation functionals for these two molecules. In Table 1 we compare the HF, DFT and MP2 results with spectroscopic data and with the recent literature CCSD(T) values for uracil. Most of the DFT results obtained for uracil and thymine with the aug-cc-pCVTZ basis set are in good agreement with the available experimental data, which may be treated as benchmark results. However, the smaller 6-311G-dp basis set results are much less satisfactory; the results are systematically too large. Similarly, much too large values are obtained at the HF level. It shows the importance of basis set and electron correlation effects for this kind of molecular properties. At the same time, the comparison with the experimental data indicates that the performance of various DFT functionals is similar, therefore we have chosen only three of them, PBE, OPTX and BPW91, for further calculations.

A comparison of the MP2 values with the experimental and CCSD(T) results indicates that for the larger basis set the electron correlation effect is overestimated at the MP2 level. We obtained similar results comparing MP2 and CCSD results for thymine using the smaller 6-311G-dp basis set. This trend is confirmed by other calculations for ^{14}N, we find that the electron correlation effect at the MP2 level is equal to ≈120% of that obtained at the CCSD(T)/aug-pCVTZ level for CH_3CN, and ≈140% for quinuclidine at the CCSD/aug-pCVDZ level [22].

3.2. Weak intermolecular forces—solvent effects

We consider first the effects due to weak solute–solvent interactions, which we describe according to one of the standard methods—using the COSMO (conductorlike screening model) [23–25]. In this model, the solvent is characterized by its dielectric constant, thus varying this parameter we obtain an approximate description of the changes of NQCC in the solute molecule for different solvents. We have chosen the uracil molecule as the solute, and selected values of the dielectric constant corresponding to vacuum, CH_2Cl_2, CH_3NO_2 and water as the solvent. The results shown in Table 2 indicate that although the vacuum values at the HF, DFT and MP2 level differ significantly, the computed solvent effect is very similar. It is practically identical in the HF and DFT approach for nitrogen nuclei, with the solvent effect determined at the MP2 level being slightly larger. For oxygen the changes due to the solvent are for each DFT functional somewhat smaller than at the HF level, and in better agreement with the MP2 results. Nevertheless, it appears that the effects caused by weak solute–solvent interactions are so small that they can be reasonably well described at any level of approximation, the main advantage of DFT and MP2 is a more reliable description of NQCCs in the solute molecule.

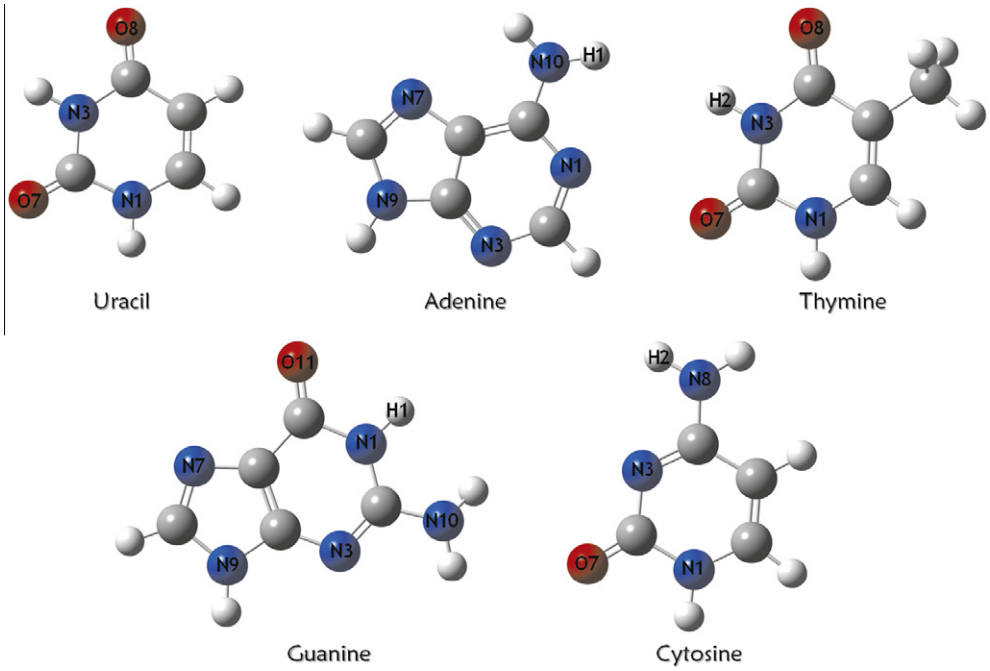

Fig. 1. Atom numbering in uracil, adenine, thymine, guanine and cytosine.

Table 1
^{14}N NQCC in uracil and thymine (in MHz).

Method	Uracil				Thymine			
	N1		N3		N1		N3	
	6-311G-dp	aug-cc-pCVTZ	6-311G-dp	aug-cc-pCVTZ	6-311G-dp	aug-cc-pCVTZ	6-311G-dp	aug-cc-pCVTZ
HF	−4.734	−4.360	−4.411	−4.041	−4.806	−4.425	−4.389	−4.024
PBE	−3.899	−3.610	−3.681	−3.387	−3.966	−3.672	−3.668	−3.379
OPTX	−3.967	−3.693	−3.755	−3.483	−4.026	−3.751	−3.737	−3.471
BPW91	−3.942	−3.679	−3.720	−3.452	−4.008	−3.740	−3.708	−3.444
BP86	−3.903	−3.624	−3.682	−3.397	−3.971	−3.687	−3.669	−3.389
PW91	−3.937	−3.644	−3.717	−3.419	−4.003	−3.706	−3.703	−3.411
OVWN	−4.109	−3.882	−3.886	−3.661	−4.167	−3.938	−3.872	−3.651
OP86	−3.828	−3.609	−3.612	−3.390	−3.891	−3.669	−3.601	−3.383
OPW91	−3.865	−3.660	−3.649	−3.442	−3.926	−3.719	−3.638	−3.434
OLYP	−3.979	−3.711	−3.761	−3.493	−4.040	−3.770	−3.746	−3.483
O3LYP	−4.207	−3.950	−3.967	−3.709	−4.269	−4.009	−3.952	−3.699
B3LYP	−4.199	−3.864	−3.954	−3.617	−4.266	−3.926	−3.935	−3.604
MP2	−4.102	−3.555	−3.822	−3.270	−4.153	−3.601	−3.800	−3.254
Exp.[a]	−3.7420(83)		−3.4505(90)		−3.804(12)		−3.420(14)	
CCSD(T)[b]	−3.691		−3.362					

[a] Uracil [14], thymine [15].
[b] Ref. [16].

Table 2
^{14}N and ^{17}O NQCC in solvated uracil (in MHz).

	Solvent				Solvent			
	Vacuum ϵ = 1.0	CH_2Cl_2 ϵ = 10.36	CH_3NO_2 ϵ = 38.2	H_2O ϵ = 78.39	Vacuum ϵ = 1.0	CH_2Cl_2 ϵ = 10.36	CH_3NO_2 ϵ = 38.2	H_2O ϵ = 78.39
	N1				N3			
HF	−4.360	−4.063	−4.019	−4.009	−4.041	−3.882	−3.863	−3.859
PBE	−3.610	−3.300	−3.253	−3.243	−3.387	−3.222	−3.202	−3.198
OPTX	−3.693	−3.396	−3.350	−3.341	−3.483	−3.323	−3.305	−3.301
BPW91	−3.679	−3.364	−3.316	−3.307	−3.452	−3.284	−3.264	−3.260
MP2	−3.555	−3.178	−3.135	−3.127	−3.270	−3.025	−3.004	−3.000
	O7				O8			
HF	−8.885	−8.488	−8.436	−8.425	−10.081	−9.404	−9.305	−9.284
PBE	−7.797	−7.555	−7.521	−7.514	−8.913	−8.442	−8.368	−8.352
OPTX	−7.852	−7.607	−7.572	−7.565	−8.930	−8.457	−8.383	−8.368
BPW91	−7.913	−7.664	−7.628	−7.621	−9.037	−8.555	−8.479	−8.463
MP2	−7.563	−7.252	−7.222	−7.217	−8.744	−8.232	−8.172	−8.161

3.3. Hydrogen bonds in nucleic acid base pairs

To examine the performance of DFT in the description of stronger intermolecular interactions, we analyzed the changes of NQCC in the presence of hydrogen bonds, choosing the adenine–thymine and guanine–cytosine pairs as an example. Studies of the potential energy surfaces for these dimers have shown that double proton transfer from the canonical structures (denoted as AT and GC) leads to the imino-enol tautomers (A*T* and G*C*), which represent energetically stable minima [10,11]. Therefore, for each dimer we analyzed two structures; we present the results for the optimized ground state geometry and for the optimized imino-enol geometry. We discuss the NQCC values for the nuclei participating in the hydrogen bonds, because for these nuclei one can expect most significant changes due to the proton transfer. The numbering of atoms for both dimers is shown in Fig. 2.

Although there are many experimental studies of NQCC in nucleic acid bases, the results primarily refer to the solid state. Therefore, the comparison of our results with experiment is not straightforward, since the type and number of hydrogen bonds in the solid state is usually different than in the studied base pairs (for instance, in the solid state NH_2 groups or oxygen atoms often participate in more than one hydrogen bond). Numerous calculations have also been done to estimate NQCC in the solid state (see e.g. Refs. [17–19,21,26]). In most of these studies DFT approach was used, and the results for isolated molecules at DFT optimized geometries are similar to ours. However, in the comparison with these theoretical data we also need to consider the role of the applied model. The systems chosen to model the solid state included usually a few molecules, with more and different hydrogen bonds than in the dimers studied in this work (consequently, also smaller basis sets have often been used). Moreover, we do not analyze the effects of the nuclear motion, which may differ significantly in the solid state and in the dimer (see. e.g, Ref. [27]). Nevertheless, we selected some literature values for the hydrogen-bonded nuclei which resemble these in the dimers, and we include the relevant data in Tables 3 and 4. For comparison with our results we selected the B3LYP results for the monomers and the experimental NQCC data for the solid state. We stress that in contrast to microwave data for monomers these results only illustrate the overall trends, they cannot be treated as accurate benchmark values for the studied dimers.

We have performed systematically all the DFT calculations for the adenine–thymine and guanine–cytosine dimers applying PBE, OPTX and BPW91 functionals. The differences between the computed NQCCs are practically negligible, thus in the discussed below comparison with other methods we report only the PBE results. We compare HF, DFT and MP2 results, because the studied dimers have 168 electrons, in the aug-pCVTZ basis set there are more than 1350 CGTOs, and thus coupled cluster calculations with this basis basis

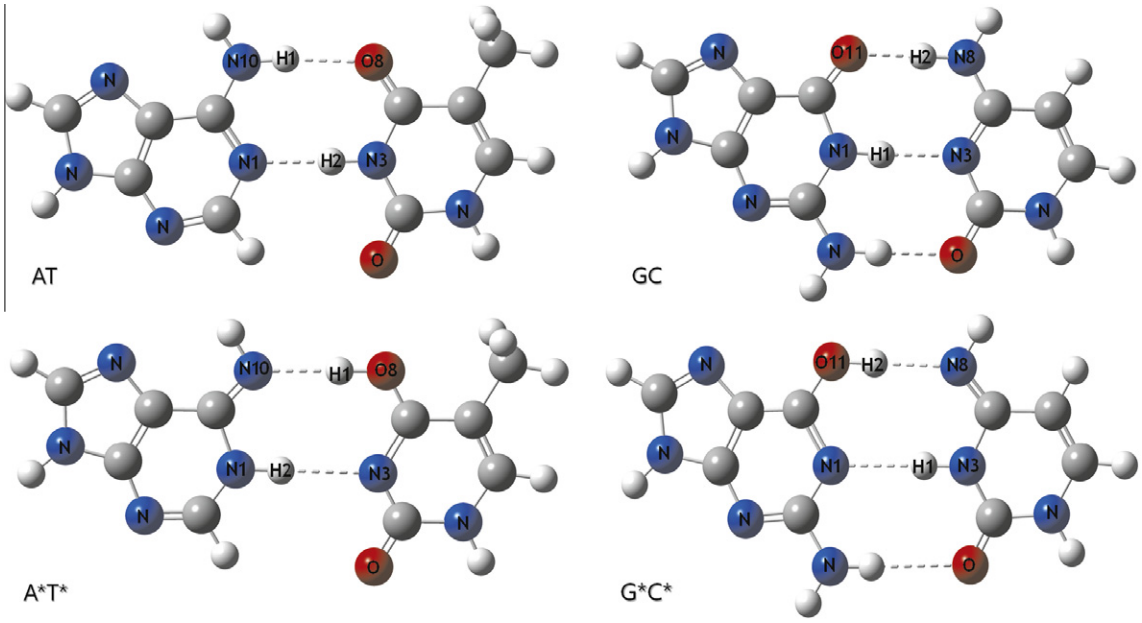

Fig. 2. Atom numbering in adenine–thymine and guanine–cytosine base pairs.

Table 3
Adenine–thymine dimer, NQCC and η of the nuclei forming the hydrogen bonds.

	Monomers			AT			A*T*		
	Adenine		Thymine						
	N10	H1	O8	N10	H1	O8	N10	H1	O8
	N–H–O bond								
NQCC									
HF	−4.748	0.271	10.167	−4.142	0.216	9.726	2.456	0.056	−8.374
PBE	−4.267	0.272	8.916	−3.665	0.219	8.508	2.169	0.081	−7.328
MP2	−4.179	0.273	8.731	−3.598	0.222	8.392	2.013	0.082	−7.097
Ref. [17][a]			8.929			8.40			
η									
HF	0.116	0.195	0.042	0.276	0.239	0.178	0.611	0.540	0.045
PBE	0.111	0.158	0.021	0.275	0.189	0.197	0.483	0.285	0.148
MP2	0.154	0.169	0.086	0.301	0.199	0.117	0.689	0.300	0.117
Ref. [17][a]			0.019			0.10			
	Adenine	Thymine							
	N1	H2	N3	N1	H2	N3	N1	H2	N3
	N–H–N bond								
NQCC									
HF	−4.207	0.254	−4.024	−3.713	0.152	−3.166	−2.431	0.147	−3.354
PBE	−3.884	0.256	−3.379	−3.344	0.161	−2.510	−1.860	0.156	−3.032
MP2	−3.878	0.265	−3.254	−3.411	0.164	−2.876	−1.644	0.159	−3.058
Ref. [18][a,b]	−4.19			−3.407					
η									
HF	0.220	0.175	0.127	0.441	0.291	0.625	0.867	0.289	0.793
PBE	0.152	0.134	0.126	0.363	0.212	0.747	0.927	0.206	0.680
MP2	0.004	0.141	0.143	0.167	0.216	0.737	0.854	0.207	0.522
Ref. [18][a]	0.182			0.335					

[a] DFT for monomers, hydrogen bonds in the solid state (see the text).
[b] Sign convention changed.

set are not practically feasible. In the guanine–cytosine dimer there are three hydrogen bonds; we shall discuss the results for the nuclei in these two which, due to proton transfer, differ in the imino-enol structure from the ground state.

The results shown in Tables 3 and 4 illustrate the role of the hydrogen bonds. Practically, for all the nuclei in the dimers the NQCCs differ significantly from the monomer values, and for each dimer the differences between the canonical and imino-enol structure are very large. We observe that the general trends are similar at each level of the calculation, and similar for the studied dimers and solid-state complexes. The formation of the hydrogen bond leads in most cases to the decrease of (the absolute value of) the NQCC for all the involved atoms, and to an increase of the anisotropy parameters. The changes of NQCC and anisotropy following the proton transfer, determined at the HF, DFT and MP2 level, are in most cases similar. For NQCC the trends differ mainly when the changes are not too large, for example in the N–H–N bonds for the N atoms in thymine and in cytosine. The differences are slightly larger for the anisotropies, with the DFT values usually between the HF and MP2 results (moreover, we observe differences

Table 4
Guanine–cytosine dimer, NQCC and η of the nuclei forming two hydrogen bonds.

	Monomers			GC			G*C*		
	Guanine	Cytosine							
	O11	H2	N8	O11	H2	N8	O11	H2	N8
	O–H–N bond								
NQCC									
HF	9.474	0.266	−4.658	8.782	0.174	−3.505	−9.248	0.166	−2.957
PBE	8.338	0.267	−4.237	7.776	0.181	−3.240	−8.242	0.182	−2.438
MP2	8.168	0.269	−4.101	7.661	0.183	−3.002	−8.064	0.185	−2.514
Ref. [19][a,b]			−3.542			−2.937			
η									
HF	0.081	0.188	0.112	0.479	0.269	0.488	0.330	0.203	0.513
PBE	0.080	0.155	0.101	0.470	0.209	0.501	0.232	0.144	0.716
MP2	0.014	0.163	0.140	0.392	0.216	0.511	0.285	0.155	0.506
Ref. [19][a]			0.110			0.378			
	Guanine		Cytosine						
	N1	H1	N3	N1	H1	N3	N1	H1	N3
	N–H–N bond								
NQCC									
HF	−4.009	0.257	−3.818	−3.431	0.181	−3.322	−3.125	0.149	−3.489
PBE	−3.496	0.259	−3.592	−2.907	0.188	−3.102	−2.764	0.158	−2.835
MP2	−3.231	0.261	−3.563	−2.848	0.205	−3.085	−2.898	0.161	−2.760
Ref. [19][a,b]			−2.767			−2.862			
Ref. [21][a,b]	−3.95			−3.610					
η									
HF	0.156	0.190	0.587	0.468	0.280	0.942	0.956	0.324	0.571
PBE	0.166	0.150	0.460	0.515	0.213	0.772	0.903	0.239	0.689
MP2	0.162	0.154	0.338	0.850	0.096	0.645	0.598	0.245	0.667
Ref. [19][a]			0.580			0.806			
Ref. [21][a]	0.14			0.37					

[a] DFT for monomers, hydrogen bonds in the solid state (see the text).
[b] Sign convention changed.

on the order of 10% between PBE, OPTX and BPW91 η values). We note that the experimental solid-state data are closer to the NQCC results for AT and GC than to the values obtained for the imino-enol A*T* and G*C* structures. Thus, it appears that the largest computed values of η (obtained for the imino-enol structures and/or at the HF level) have no physical meaning.

To estimate the role of different factors contributing to the change of NQCCs we performed additional calculations for adenine and thymine at the geometries taken from the AT dimer structure, using the COSMO model. As expected, in general the results do not reproduce the AT dimer values. The noticeable differences with respect to the monomers, observed already in vacuum (thus due to geometry changes) are for the hydrogen nuclei—the NQCCs decrease, and the asymmetry parameters increase, in agreement with the trends shown in Table 3.

3.4. Hexamine-3phenol complex—hydrogen bonds in the solid state

We have recently computed nitrogen NQCC in isolated hexamine (hexamethylenetetramine, $(CH_2)_6N_4$) [22]. The nuclear quadrupole coupling in hexamine and its complexes has been analyzed applying different experimental techniques [28–30], therefore as a practical model to study the effects of hydrogen bonding in the solid state we have chosen the hexamine-3phenol complex—three nitrogen atoms form identical bonds, whereas the last one remains non-bonded. We determined the structure of the complex beginning with the experimental data [31], and then optimizing the geometry at the DFT/B3LYP/6-311G-dp level, while maintaining the C_3 propeller symmetry (see Fig. 3). The NQCC values discussed below were next computed at this optimized geometry using the aug-cc-pCVTZ basis set.

We have analyzed previously the electron correlation effects on NQCC in hexamine, comparing HF, DFT and CCSD results [22]. This

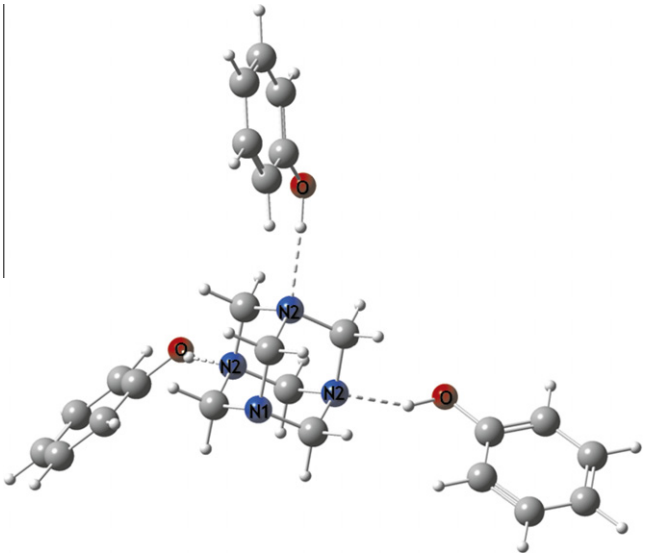

Fig. 3. Hexamine-3phenol complex.

analysis indicated that most DFT functionals underestimate the electron correlation effects; although PBE, OPTX and BPW91 approaches recover a significant part of the correlation effects this can also be observed comparing the HF, DFT and experimental results for N (0) in Table 5. The description of the changes of NQCC in the complex is not systematically improved. For the nonbonded nitrogen, all the DFT values of N (1) – N (0) are slightly closer to the experimental value than the HF result, but for the nuclei participating in the hydrogen bond the DFT values of N (2) – N (0) are, just like the HF result, in qualitative rather than quantitative agreement with experiment. We can also compare with experimental

Table 5
^{14}N NQCC in hexamine–3phenol complex (in MHz).[a]

	Hexamine-3phenol		Hexamine	Differences	
	N (1)	N (2)	N (0)	N (1) − N (0)	N (2) − N (0)
HF	−5.486	−5.060	−5.327	−0.160	0.266
PBE	−4.979	−4.453	−4.826	−0.153	0.373
OPTX	−4.951	−4.545	−4.795	−0.156	0.250
BPW91	−5.054	−4.514	−4.905	−0.150	0.391
Exp.[b]	−4.6657	−4.2081	−4.5343	−0.1314	0.3262

[a] Following Ref. [28], N (0) denotes the hexamine nitrogen, N (1) the non-bonded nitrogen in the complex and N (2) the nucleus participating in the hydrogen bond.
[b] Ref. [28] (at 77 K, sign convention changed).

data the asymmetry of the tensor, we have $\eta_{N0} = \eta_{N1} = 0$ by symmetry and the non-zero experimental value is $\eta_{N2} = 0.05014$ [28]. The calculated values of η_{N2} are too small, we obtain 0.009 at the HF level and 0.016–0.017 for DFT functionals. However, the discrepancies between theory and experiment for N (2) − N (0) and η_{N2} may be due to the deficiency of the chosen structure of the complex (the experimental value is for the solid state), rather than due to the approximations in the final DFT calculations of NQCCs.

4. Conclusions

Accurate ab initio calculations of nuclear quadrupole coupling constants, which provide reliable results, become feasible for small polyatomic molecules. However, it is not yet possible to apply the most advanced methods to describe the role of intermolecular interactions. In the analysis of electron correlation effects we have therefore compared DFT results with MP2, even though monomer calculations indicate that in many cases the MP2 approach overestimates the correlation correction. The computed changes in NQCC due to intermolecular interactions do not depend significantly on the level of approximation, the trends are the same in the HF, DFT and MP2 approach (in particular, they are practically independent of the exchange–correlation functional, at least for the functionals applied in this study). In the studied systems, the changes of NQCC were related to the formation of intermolecular hydrogen bonds. In most cases, the absolute values of the NQCCs decreased and the anisotropies increased with respect to the isolated molecule values for all the nuclei participating in the hydrogen bonds.

To summarize, the description of the nuclear quadrupole coupling at the DFT level is of qualitative rather than quantitative accuracy. Nevertheless we observe that, like for many other molecular properties, DFT provides a useful approach to estimate the effects of intermolecular forces. In particular, the changes of NQCCs due to hydrogen bonds, computed with the DFT and MP2 approaches, do not differ significantly. Therefore, an efficient scheme for comparison of computed and experimental results is to determine the results for the isolated molecule at the best possible level of approximation—for instance, at the coupled cluster level—and to add small corrections describing the role of intermolecular forces determined at the DFT level.

Acknowledgments

We are indebted to Prof. Joanna Sadlej for her comments on the manuscript. This work was supported by Polish MNiSW Grant N N204 189938.

References

[1] S.P.A. Sauer, Molecular Electromagnetism, A Computational Chemistry Approach, Oxford University Press, Oxford, 2011.
[2] J. Bieroń, P. Pyykkö, D. Sundholm, V. Kellö, A.J. Sadlej, Nuclear quadrupole moments of bromine and iodine from combined atomic and molecular data, Phys. Rev. A 64 (2001) 052507. 1-12.
[3] V. Kellö, A.J. Sadlej, The nuclear quadrupole moment of ^{14}N from accurate electric field gradient calculations and microwave spectra of NP molecule, Collect. Czech. Chem. Commun. 72 (2007) 64–82.
[4] W.C. Bailey, DFT and HF–DFT calculations of ^{14}N quadrupole coupling constants in molecules, Chem. Phys. 252 (2000) 57–66.
[5] W.C. Bailey, <http://turbo.kean.edu/~wbailey/Nitrogen.html>.
[6] P. Pyykkö, Year-2008 nuclear quadrupole moments, Mol. Phys. 106 (2008) 1965–1974.
[7] PQS version 3.3, Parallel Quantum Solutions 2013 Green Acres Road, Fayetteville, Arkansas 72703, <http://www.pqs-chem.com>.
[8] M.J. Frisch, G.W. Trucks, H.B. Schlegel, G.E. Scuseria, M.A. Robb, J.R. Cheeseman, G. Scalmani, V. Barone, B. Mennucci, G.A. Petersson, H. Nakatsuji, M. Caricato, X. Li, H.P. Hratchian, A.F. Izmaylov, J. Bloino, G. Zheng, J.L. Sonnenberg, M. Hada, M. Ehara, K. Toyota, R. Fukuda, J. Hasegawa, M. Ishida, T. Nakajima, Y. Honda, O. Kitao, H. Nakai, T. Vreven, J.A. Montgomery, Jr., J.E. Peralta, F. Ogliaro, M. Bearpark, J.J. Heyd, E. Brothers, K.N. Kudin, V.N. Staroverov, R. Kobayashi, J. Normand, K. Raghavachari, A. Rendell, J.C. Burant, S.S. Iyengar, J. Tomasi, M. Cossi, N. Rega, J.M. Millam, M. Klene, J.E. Knox, J.B. Cross, V. Bakken, C. Adamo, J. Jaramillo, R. Gomperts, R.E. Stratmann, O. Yazyev, A.J. Austin, R. Cammi, C. Pomelli, J.W. Ochterski, R.L. Martin, K. Morokuma, V.G. Zakrzewski, G.A. Voth, P. Salvador, J.J. Dannenberg, S. Dapprich, A.D. Daniels, O. Farkas, J.B. Foresman, J.V. Ortiz, J. Cioslowski, D.J. Fox, Gaussian 09 Revision A.1, Gaussian Inc. Wallingford, CT, 2009.
[9] CFOUR, A quantum chemical program package written by J.F. Stanton, J. Gauss, M.E. Harding, P.G. Szalay with contributions from A.A. Auer, R.J. Bartlett, U. Benedikt, C. Berger, D.E. Bernholdt, O. Christiansen, M. Heckert, O. Heun, C. Huber, D. Jonsson, J. Jusélius, K. Klein, W.J. Lauderdale, D. Matthews, T. Metzroth, D.P. O'Neill, D.R. Price, E. Prochnow, K. Ruud, F. Schiffmann, S. Stopkowicz, A. Tajti, M.E. Varner, J. Vázquez, F. Wang, J.D. Watts and the integral packages MOLECULE (J. Almlöf and P.R. Taylor), PROPS (P.R. Taylor), ABACUS (T. Helgaker, H.J. Aa. Jensen, P. Jørgensen, J. Olsen), and ECP routines by A.V. Mitin, C. van Wüllen. For the current version, see <http://www.cfour.de>.
[10] J. Florián, V. Hrouda, P. Hobza, Proton transfer in the adenine–thymine base pair, J. Am. Chem. Soc. 116 (1994) 1457–1460.
[11] J. Florián, J. Leszczyński, S. Scheiner, Ab initio study of the structure of guanine–cytosine base pair conformers in gas phase and polar solvents, Mol. Phys. 84 (1995) 469–480.
[12] N. Russo, E. Sicilia, M. Toscano, A. Grand, Theoretical prediction of nuclear quadrupole coupling constants of DNA and RNA nucleic acid bases, J. Mol. Struct. 563–564 (2001) 125–134.
[13] S. Brünken, M.C. McCarthy, P. Thaddeus, P.D. Godfrey, R.D. Brown, Improved line frequencies for the nucleic acid base uracil for a radioastronomical search, Astron. Astrophys. 459 (2006) 317–320.
[14] V. Vaquero, M.E. Sanz, J.C. López, J.L. Alonso, The structure of uracil: a laser ablation rotational study, J. Phys. Chem. A 111 (2007) 3443–3445.
[15] J.C. López, M.I. Peña, M.E. Sanz, J.L. Alonso, Probing thymine with laser ablation molecular beam Fourier transform microwave spectroscopy, J. Chem. Phys. 126 (2007) 191103. 1-4.
[16] C. Puzzarini, V. Barone, Extending the molecular size in accurate quantum-chemical calculations: the equilibrium structure and spectroscopic properties of uracil, Phys. Chem. Chem. Phys. 13 (2011) 7189–7197.
[17] G. Wu, S. Dong, R. Ida, N. Reen, A solid-state ^{17}O nuclear magnetic resonance study of nucleic acid bases, J. Am. Chem. Soc. 124 (2002) 1768–1777.
[18] M. Mirzaei, N.L. Hadipour, An investigation of hydrogen-bonding effects on the nitrogen and hydrogen electric field gradient and chemical shielding tensors In the 9-methyladenine real crystalline structure: a density functional theory study, J. Phys. Chem. A 110 (2006) 4833–4838.
[19] J.N. Latosińska, M. Latosińska, J. Koput, The tautomeric equilibria of cytosine studied by NQR spectroscopy and HF, MP2 and DFT calculations, J. Mol. Struct. 648 (2003) 9–18.
[20] M. Mirzaei, N.L. Hadipour, K. Ahmadi, Investigation of C–H···O = C and N–H···O = C hydrogen-bonding interactions in crystalline thymine by DFT calculations of O-17, N-14 and H-2 NQR parameters, Biophys. Chem. 125 (2007) 411–415.
[21] M. Monajjemi, B. Honarparvar, S.M. Nasseri, M. Khalegian, NQR and NMR study of hydrogen bonding interactions in anhydrous and monohydrated guanine cluster model: a computational study, J. Struct. Chem. 50 (2009) 67–77.
[22] A. Brzyska, M. Jaszuński, Coupled cluster and DFT calculations of ^{14}N nuclear quadrupole coupling constants, Int. J. Quantum Chem. (2011), doi:10.1002/qua.23180.
[23] A. Klamt, G. Schüürmann, COSMO: a new approach to dielectric screening in solvents with explicit expressions for the screening energy and its gradient, J. Chem. Soc., Perkin Trans. 2 (1993) 799–805.
[24] A. Klamt, Conductor-like screening model for real solvents: a new approach to the quantitative calculation of solvation phenomena, J. Phys. Chem. 99 (1995) 2224–2235.
[25] A. Klamt, V. Jones, Treatment of the outlying charge in continuum solvation models, J. Chem. Phys. 105 (1996) 9972–9982.
[26] E. Zahedi, M. Aghaie, K. Zare, A density functional study of NBO, NICS and ^{14}N NQR parameters of 5-methylcytosine tautomers in the gas phase, J. Mol. Struct. (THEOCHEM) 905 (2009) 101–105.
[27] P. Pyykkö, F. Elmi, Deuteron quadrupole coupling in benzene: librational corrections using a temperature-dependent Einstein model, and summary. The symmetries of electric field gradients and conditions for $\eta = 1$, Phys. Chem. Chem. Phys. 10 (2008) 3867–3871.

[28] R.A. Marino, ^{14}N quadrupole resonance study of a hydrogen bond: hexamethylenetetramine triphenol, J. Chem. Phys. 57 (1972) 4560–4563.
[29] B. Ancian, B. Tiffon, Multinuclear magnetic relaxation determination of nuclear quadrupole coupling constants for adamantane and hexamethylenetetramine in solution, J. Chem. Soc. Faraday Trans. 2 80 (1984) 1067–1076.
[30] J. Murgich, R. Magaly Santana, O.E. Diaz, Nuclear quadrupole resonance study of some hydrogen-bonded complexes of hexamethylenetetramine, J. Magn. Reson. 51 (1983) 26–36.
[31] T.H. Jordan, T.C.W. Mak, Molecular and crystal structure of hexamethylenetetramine triphenol, J. Chem. Phys. 52 (1970) 3790–3794.